BABAR-CONF-02/015
SLAC-PUB-9298-Rev1
hep-ex/0207058
May 2003

A Study of Time-Dependent *CP* Asymmetry in $B^0 \to J/\psi\,\pi^0$ Decays

The *BABAR* Collaboration

July 24, 2002

Abstract

We present our first study of the time-dependent *CP*-violating asymmetry in $B^0 \to J/\psi\,\pi^0$ decays using e^+e^- annihilation data collected with the *BABAR* detector at the $\Upsilon(4S)$ resonance during the years 1999–2002 at the PEP-II asymmetric-energy B Factory at SLAC. With about 88 million $B\overline{B}$ pairs, our preliminary results for the coefficients of the cosine and sine terms of the *CP* asymmetry are $C_{J/\psi\,\pi^0} = 0.38 \pm 0.41\ \text{(stat)} \pm 0.09\ \text{(syst)}$ and $S_{J/\psi\,\pi^0} = 0.05 \pm 0.49\ \text{(stat)} \pm 0.16\ \text{(syst)}$.

Contributed to the 31^{st} International Conference on High Energy Physics,
7/24—7/31/2002, Amsterdam, The Netherlands

Stanford Linear Accelerator Center, Stanford University, Stanford, CA 94309

Work supported in part by Department of Energy contract DE-AC03-76SF00515.

The *BABAR* Collaboration,

B. Aubert, D. Boutigny, J.-M. Gaillard, A. Hicheur, Y. Karyotakis, J. P. Lees, P. Robbe, V. Tisserand, A. Zghiche

Laboratoire de Physique des Particules, F-74941 Annecy-le-Vieux, France

A. Palano, A. Pompili

Università di Bari, Dipartimento di Fisica and INFN, I-70126 Bari, Italy

J. C. Chen, N. D. Qi, G. Rong, P. Wang, Y. S. Zhu

Institute of High Energy Physics, Beijing 100039, China

G. Eigen, I. Ofte, B. Stugu

University of Bergen, Inst. of Physics, N-5007 Bergen, Norway

G. S. Abrams, A. W. Borgland, A. B. Breon, D. N. Brown, J. Button-Shafer, R. N. Cahn, E. Charles, M. S. Gill, A. V. Gritsan, Y. Groysman, R. G. Jacobsen, R. W. Kadel, J. Kadyk, L. T. Kerth, Yu. G. Kolomensky, J. F. Kral, C. LeClerc, M. E. Levi, G. Lynch, L. M. Mir, P. J. Oddone, T. J. Orimoto, M. Pripstein, N. A. Roe, A. Romosan, M. T. Ronan, V. G. Shelkov, A. V. Telnov, W. A. Wenzel

Lawrence Berkeley National Laboratory and University of California, Berkeley, CA 94720, USA

T. J. Harrison, C. M. Hawkes, D. J. Knowles, S. W. O'Neale, R. C. Penny, A. T. Watson, N. K. Watson

University of Birmingham, Birmingham, B15 2TT, United Kingdom

T. Deppermann, K. Goetzen, H. Koch, B. Lewandowski, K. Peters, H. Schmuecker, M. Steinke

Ruhr Universität Bochum, Institut für Experimentalphysik 1, D-44780 Bochum, Germany

N. R. Barlow, W. Bhimji, J. T. Boyd, N. Chevalier, P. J. Clark, W. N. Cottingham, C. Mackay, F. F. Wilson

University of Bristol, Bristol BS8 1TL, United Kingdom

K. Abe, C. Hearty, T. S. Mattison, J. A. McKenna, D. Thiessen

University of British Columbia, Vancouver, BC, Canada V6T 1Z1

S. Jolly, A. K. McKemey

Brunel University, Uxbridge, Middlesex UB8 3PH, United Kingdom

V. E. Blinov, A. D. Bukin, A. R. Buzykaev, V. B. Golubev, V. N. Ivanchenko, A. A. Korol, E. A. Kravchenko, A. P. Onuchin, S. I. Serednyakov, Yu. I. Skovpen, A. N. Yushkov

Budker Institute of Nuclear Physics, Novosibirsk 630090, Russia

D. Best, M. Chao, D. Kirkby, A. J. Lankford, M. Mandelkern, S. McMahon, D. P. Stoker

University of California at Irvine, Irvine, CA 92697, USA

C. Buchanan, S. Chun

University of California at Los Angeles, Los Angeles, CA 90024, USA

H. K. Hadavand, E. J. Hill, D. B. MacFarlane, H. Paar, S. Prell, Sh. Rahatlou, G. Raven, U. Schwanke, V. Sharma

University of California at San Diego, La Jolla, CA 92093, USA

J. W. Berryhill, C. Campagnari, B. Dahmes, P. A. Hart, N. Kuznetsova, S. L. Levy, O. Long, A. Lu, M. A. Mazur, J. D. Richman, W. Verkerke

University of California at Santa Barbara, Santa Barbara, CA 93106, USA

J. Beringer, A. M. Eisner, M. Grothe, C. A. Heusch, W. S. Lockman, T. Pulliam, T. Schalk, R. E. Schmitz, B. A. Schumm, A. Seiden, M. Turri, W. Walkowiak, D. C. Williams, M. G. Wilson

University of California at Santa Cruz, Institute for Particle Physics, Santa Cruz, CA 95064, USA

E. Chen, G. P. Dubois-Felsmann, A. Dvoretskii, D. G. Hitlin, F. C. Porter, A. Ryd, A. Samuel, S. Yang

California Institute of Technology, Pasadena, CA 91125, USA

S. Jayatilleke, G. Mancinelli, B. T. Meadows, M. D. Sokoloff

University of Cincinnati, Cincinnati, OH 45221, USA

T. Barillari, P. Bloom, W. T. Ford, U. Nauenberg, A. Olivas, P. Rankin, J. Roy, J. G. Smith, W. C. van Hoek, L. Zhang

University of Colorado, Boulder, CO 80309, USA

J. L. Harton, T. Hu, M. Krishnamurthy, A. Soffer, W. H. Toki, R. J. Wilson, J. Zhang

Colorado State University, Fort Collins, CO 80523, USA

D. Altenburg, T. Brandt, J. Brose, T. Colberg, M. Dickopp, R. S. Dubitzky, A. Hauke, E. Maly, R. Müller-Pfefferkorn, S. Otto, K. R. Schubert, R. Schwierz, B. Spaan, L. Wilden

Technische Universität Dresden, Institut für Kern- und Teilchenphysik, D-01062 Dresden, Germany

D. Bernard, G. R. Bonneaud, F. Brochard, J. Cohen-Tanugi, S. Ferrag, S. T'Jampens, Ch. Thiebaux, G. Vasileiadis, M. Verderi

Ecole Polytechnique, LLR, F-91128 Palaiseau, France

A. Anjomshoaa, R. Bernet, A. Khan, D. Lavin, F. Muheim, S. Playfer, J. E. Swain, J. Tinslay

University of Edinburgh, Edinburgh EH9 3JZ, United Kingdom

M. Falbo

Elon University, Elon University, NC 27244-2010, USA

C. Borean, C. Bozzi, L. Piemontese, A. Sarti

Università di Ferrara, Dipartimento di Fisica and INFN, I-44100 Ferrara, Italy

E. Treadwell

Florida A&M University, Tallahassee, FL 32307, USA

F. Anulli,[1] R. Baldini-Ferroli, A. Calcaterra, R. de Sangro, D. Falciai, G. Finocchiaro, P. Patteri, I. M. Peruzzi,[1] M. Piccolo, A. Zallo

Laboratori Nazionali di Frascati dell'INFN, I-00044 Frascati, Italy

S. Bagnasco, A. Buzzo, R. Contri, G. Crosetti, M. Lo Vetere, M. Macri, M. R. Monge, S. Passaggio, F. C. Pastore, C. Patrignani, E. Robutti, A. Santroni, S. Tosi

Università di Genova, Dipartimento di Fisica and INFN, I-16146 Genova, Italy

[1]Also with Università di Perugia, I-06100 Perugia, Italy

S. Bailey, M. Morii
Harvard University, Cambridge, MA 02138, USA

R. Bartoldus, G. J. Grenier, U. Mallik
University of Iowa, Iowa City, IA 52242, USA

J. Cochran, H. B. Crawley, J. Lamsa, W. T. Meyer, E. I. Rosenberg, J. Yi
Iowa State University, Ames, IA 50011-3160, USA

M. Davier, G. Grosdidier, A. Höcker, H. M. Lacker, S. Laplace, F. Le Diberder, V. Lepeltier, A. M. Lutz, T. C. Petersen, S. Plaszczynski, M. H. Schune, L. Tantot, S. Trincaz-Duvoid, G. Wormser
Laboratoire de l'Accélérateur Linéaire, F-91898 Orsay, France

R. M. Bionta, V. Brigljević , D. J. Lange, K. van Bibber, D. M. Wright
Lawrence Livermore National Laboratory, Livermore, CA 94550, USA

A. J. Bevan, J. R. Fry, E. Gabathuler, R. Gamet, M. George, M. Kay, D. J. Payne, R. J. Sloane, C. Touramanis
University of Liverpool, Liverpool L69 3BX, United Kingdom

M. L. Aspinwall, D. A. Bowerman, P. D. Dauncey, U. Egede, I. Eschrich, G. W. Morton, J. A. Nash, P. Sanders, D. Smith, G. P. Taylor
University of London, Imperial College, London, SW7 2BW, United Kingdom

J. J. Back, G. Bellodi, P. Dixon, P. F. Harrison, R. J. L. Potter, H. W. Shorthouse, P. Strother, P. B. Vidal
Queen Mary, University of London, E1 4NS, United Kingdom

G. Cowan, H. U. Flaecher, S. George, M. G. Green, A. Kurup, C. E. Marker, T. R. McMahon, S. Ricciardi, F. Salvatore, G. Vaitsas, M. A. Winter
University of London, Royal Holloway and Bedford New College, Egham, Surrey TW20 0EX, United Kingdom

D. Brown, C. L. Davis
University of Louisville, Louisville, KY 40292, USA

J. Allison, R. J. Barlow, A. C. Forti, F. Jackson, G. D. Lafferty, A. J. Lyon, N. Savvas, J. H. Weatherall, J. C. Williams
University of Manchester, Manchester M13 9PL, United Kingdom

A. Farbin, A. Jawahery, V. Lillard, D. A. Roberts, J. R. Schieck
University of Maryland, College Park, MD 20742, USA

G. Blaylock, C. Dallapiccola, K. T. Flood, S. S. Hertzbach, R. Kofler, V. B. Koptchev, T. B. Moore, H. Staengle, S. Willocq
University of Massachusetts, Amherst, MA 01003, USA

B. Brau, R. Cowan, G. Sciolla, F. Taylor, R. K. Yamamoto
Massachusetts Institute of Technology, Laboratory for Nuclear Science, Cambridge, MA 02139, USA

M. Milek, P. M. Patel
McGill University, Montréal, QC, Canada H3A 2T8

F. Palombo

Università di Milano, Dipartimento di Fisica and INFN, I-20133 Milano, Italy

J. M. Bauer, L. Cremaldi, V. Eschenburg, R. Kroeger, J. Reidy, D. A. Sanders, D. J. Summers

University of Mississippi, University, MS 38677, USA

C. Hast, P. Taras

Université de Montréal, Laboratoire René J. A. Lévesque, Montréal, QC, Canada H3C 3J7

H. Nicholson

Mount Holyoke College, South Hadley, MA 01075, USA

C. Cartaro, N. Cavallo, G. De Nardo, F. Fabozzi, C. Gatto, L. Lista, P. Paolucci, D. Piccolo, C. Sciacca

Università di Napoli Federico II, Dipartimento di Scienze Fisiche and INFN, I-80126, Napoli, Italy

J. M. LoSecco

University of Notre Dame, Notre Dame, IN 46556, USA

J. R. G. Alsmiller, T. A. Gabriel

Oak Ridge National Laboratory, Oak Ridge, TN 37831, USA

J. Brau, R. Frey, M. Iwasaki, C. T. Potter, N. B. Sinev, D. Strom, E. Torrence

University of Oregon, Eugene, OR 97403, USA

F. Colecchia, A. Dorigo, F. Galeazzi, M. Margoni, M. Morandin, M. Posocco, M. Rotondo, F. Simonetto, R. Stroili, C. Voci

Università di Padova, Dipartimento di Fisica and INFN, I-35131 Padova, Italy

M. Benayoun, H. Briand, J. Chauveau, P. David, Ch. de la Vaissière, L. Del Buono, O. Hamon, Ph. Leruste, J. Ocariz, M. Pivk, L. Roos, J. Stark

Universités Paris VI et VII, Lab de Physique Nucléaire H. E., F-75252 Paris, France

P. F. Manfredi, V. Re, V. Speziali

Università di Pavia, Dipartimento di Elettronica and INFN, I-27100 Pavia, Italy

L. Gladney, Q. H. Guo, J. Panetta

University of Pennsylvania, Philadelphia, PA 19104, USA

C. Angelini, G. Batignani, S. Bettarini, M. Bondioli, F. Bucci, G. Calderini, E. Campagna, M. Carpinelli, F. Forti, M. A. Giorgi, A. Lusiani, G. Marchiori, F. Martinez-Vidal, M. Morganti, N. Neri, E. Paoloni, M. Rama, G. Rizzo, F. Sandrelli, G. Triggiani, J. Walsh

Università di Pisa, Scuola Normale Superiore and INFN, I-56010 Pisa, Italy

M. Haire, D. Judd, K. Paick, L. Turnbull, D. E. Wagoner

Prairie View A&M University, Prairie View, TX 77446, USA

J. Albert, G. Cavoto,[2] N. Danielson, P. Elmer, C. Lu, V. Miftakov, J. Olsen, S. F. Schaffner, A. J. S. Smith, A. Tumanov, E. W. Varnes

Princeton University, Princeton, NJ 08544, USA

[2]Also with Università di Roma La Sapienza, Roma, Italy

F. Bellini, D. del Re, R. Faccini,[3] F. Ferrarotto, F. Ferroni, E. Leonardi, M. A. Mazzoni, S. Morganti, G. Piredda, F. Safai Tehrani, M. Serra, C. Voena

Università di Roma La Sapienza, Dipartimento di Fisica and INFN, I-00185 Roma, Italy

S. Christ, G. Wagner, R. Waldi

Universität Rostock, D-18051 Rostock, Germany

T. Adye, N. De Groot, B. Franek, N. I. Geddes, G. P. Gopal, S. M. Xella

Rutherford Appleton Laboratory, Chilton, Didcot, Oxon, OX11 0QX, United Kingdom

R. Aleksan, S. Emery, A. Gaidot, P.-F. Giraud, G. Hamel de Monchenault, W. Kozanecki, M. Langer, G. W. London, B. Mayer, G. Schott, B. Serfass, G. Vasseur, Ch. Yeche, M. Zito

DAPNIA, Commissariat à l'Energie Atomique/Saclay, F-91191 Gif-sur-Yvette, France

M. V. Purohit, A. W. Weidemann, F. X. Yumiceva

University of South Carolina, Columbia, SC 29208, USA

I. Adam, D. Aston, N. Berger, A. M. Boyarski, M. R. Convery, D. P. Coupal, D. Dong, J. Dorfan, W. Dunwoodie, R. C. Field, T. Glanzman, S. J. Gowdy, E. Grauges , T. Haas, T. Hadig, V. Halyo, T. Himel, T. Hryn'ova, M. E. Huffer, W. R. Innes, C. P. Jessop, M. H. Kelsey, P. Kim, M. L. Kocian, U. Langenegger, D. W. G. S. Leith, S. Luitz, V. Luth, H. L. Lynch, H. Marsiske, S. Menke, R. Messner, D. R. Muller, C. P. O'Grady, V. E. Ozcan, A. Perazzo, M. Perl, S. Petrak, H. Quinn, B. N. Ratcliff, S. H. Robertson, A. Roodman, A. A. Salnikov, T. Schietinger, R. H. Schindler, J. Schwiening, G. Simi, A. Snyder, A. Soha, S. M. Spanier, J. Stelzer, D. Su, M. K. Sullivan, H. A. Tanaka, J. Va'vra, S. R. Wagner, M. Weaver, A. J. R. Weinstein, W. J. Wisniewski, D. H. Wright, C. C. Young

Stanford Linear Accelerator Center, Stanford, CA 94309, USA

P. R. Burchat, C. H. Cheng, T. I. Meyer, C. Roat

Stanford University, Stanford, CA 94305-4060, USA

R. Henderson

TRIUMF, Vancouver, BC, Canada V6T 2A3

W. Bugg, H. Cohn

University of Tennessee, Knoxville, TN 37996, USA

J. M. Izen, I. Kitayama, X. C. Lou

University of Texas at Dallas, Richardson, TX 75083, USA

F. Bianchi, M. Bona, D. Gamba

Università di Torino, Dipartimento di Fisica Sperimentale and INFN, I-10125 Torino, Italy

L. Bosisio, G. Della Ricca, S. Dittongo, L. Lanceri, P. Poropat, L. Vitale, G. Vuagnin

Università di Trieste, Dipartimento di Fisica and INFN, I-34127 Trieste, Italy

R. S. Panvini

Vanderbilt University, Nashville, TN 37235, USA

[3]Also with University of California at San Diego, La Jolla, CA 92093, USA

S. W. Banerjee, C. M. Brown, D. Fortin, P. D. Jackson, R. Kowalewski, J. M. Roney
University of Victoria, Victoria, BC, Canada V8W 3P6

H. R. Band, S. Dasu, M. Datta, A. M. Eichenbaum, H. Hu, J. R. Johnson, R. Liu, F. Di Lodovico, A. Mohapatra, Y. Pan, R. Prepost, I. J. Scott, S. J. Sekula, J. H. von Wimmersperg-Toeller, J. Wu, S. L. Wu, Z. Yu
University of Wisconsin, Madison, WI 53706, USA

H. Neal
Yale University, New Haven, CT 06511, USA

1 Introduction

The Standard Model of electroweak interactions describes *CP*-violation in B meson decays by a complex phase in the three-generation Cabibbo-Kobayashi-Maskawa (CKM) [1] quark-mixing matrix. The $b \to c\overline{c}s$ modes that decay through charmonium, such as $B^0 \to J/\psi K^0_S$, yield precise measurements of the quantity $\sin 2\beta$, where $\beta \equiv \arg\left[-V_{\rm cd}V^*_{\rm cb}/V_{\rm td}V^*_{\rm tb}\right]$ (see for example Refs. [2, 3, 4]). The decay $B^0 \to J/\psi\pi^0$ is a Cabibbo-suppressed $b \to c\overline{c}d$ decay, whose tree contribution has the same weak phase as the $b \to c\overline{c}s$ modes (e.g. $B^0 \to J/\psi K^0_S$). A portion of the penguin contribution has a different weak phase, which may give a time-dependent *CP* asymmetry that differs from the one observed in $b \to c\overline{c}s$ decays.

In this measurement, about 88 million $\Upsilon(4S) \to B\overline{B}$ decays are used to detect the decay chain $B^0 \to J/\psi\pi^0$, with $J/\psi \to e^+e^-$ or $J/\psi \to \mu^+\mu^-$. The *BABAR* measurement of the $B^0 \to J/\psi\pi^0$ branching fraction, $(2.0 \pm 0.6\ (\mathrm{stat}) \pm 0.2\ (\mathrm{syst})) \times 10^{-5}$, is described elsewhere [5]. Properties of the recoiling B meson are used to infer the flavor (B^0 or $\overline{B}^0$) of the B meson that is reconstructed from J/ψ and π^0 candidates. The decay time distribution of B decays to a *CP* eigenstate with a B^0 or $\overline{B}^0$ flavor tag can be expressed in terms of a complex parameter λ that depends on both the B^0-$\overline{B}^0$ oscillation amplitude and the amplitudes describing $\overline{B}^0$ and B^0 decays to this final state [6]. The decay rate $\mathrm{f}_+(\mathrm{f}_-)$ when the tagging meson is a $B^0(\overline{B}^0)$ is given by

$$\mathrm{f}_\pm(\Delta t) = \frac{e^{-|\Delta t|/\tau_{B^0}}}{4\tau_{B^0}} \times \left[1 \pm \frac{2\mathcal{I}m\lambda}{1+|\lambda|^2}\sin(\Delta m_d\Delta t) \mp \frac{1-|\lambda|^2}{1+|\lambda|^2}\cos(\Delta m_d\Delta t)\right], \tag{1}$$

where $\Delta t = t_{\rm rec} - t_{\rm tag}$ is the difference between the proper decay time of the reconstructed B meson ($B_{\rm rec}$) and the proper decay time of the tagging B meson ($B_{\rm tag}$), τ_{B^0} is the B^0 lifetime, and Δm_d is the B^0-$\overline{B}^0$ oscillation frequency. The sine term in Eq. 1 is due to the interference between direct decay and decay after flavor change, and the cosine term is due to the interference between two or more decay amplitudes with different weak and strong phases. Two amplitudes can contribute in the decay $B^0 \to J/\psi\pi^0$. A portion of the penguin amplitude has the same weak phase as the tree amplitude, while the remainder of the penguin amplitude has a different weak phase. In $b \to c\overline{c}d$ decays, the tree contribution is Cabibbo-suppressed and the penguin and tree diagrams may enter at the same order, proportional to λ^3 (where in this case λ is the Wolfenstein parameter of the CKM matrix, rather than the complex parameter that appears in Eq. 1). Evidence for *CP* violation can be observed as a difference between the Δt distributions of B^0- and $\overline{B}^0$-tagged events or as an asymmetry with respect to $\Delta t = 0$ for either flavor tag. We measure the two asymmetry coefficients, defined as

$$S_f \equiv \frac{2\mathcal{I}m\lambda}{1+|\lambda|^2} \qquad \text{and} \qquad C_f \equiv \frac{1-|\lambda|^2}{1+|\lambda|^2}, \tag{2}$$

where f is the final state. With these definitions, the absence of penguin contributions would give $S_{J/\psi\pi^0} = -\sin 2\beta$ and $C_{J/\psi\pi^0} = 0$. A statistically significant deviation from these values may indicate penguin contributions not only in $B^0 \to J/\psi\pi^0$, but also in $B^0 \to J/\psi K^0_S$ (at a reduced level governed by Cabibbo suppression).

2 The *BABAR* detector and dataset

The data used in this measurement were collected with the *BABAR* detector at the PEP-II storage ring from 1999 to 2002. Approximately 81 fb^{-1} of e^+e^- annihilation data taken at the $\Upsilon(4S)$ resonance are used, corresponding to a sample of about 88 million $B\overline{B}$ pairs. An additional 5 fb^{-1} of data collected approximately 40 MeV below the $\Upsilon(4S)$ resonance are used to characterize one of the background sources.

The *BABAR* detector is described in detail elsewhere [7]. Surrounding the beam pipe is a silicon vertex tracker (SVT), which provides precise measurements of the trajectories of charged particles as they leave the e^+e^- interaction point. A 40-layer drift chamber (DCH) surrounds the SVT, and both allow measurements of track momenta in a 1.5-T magnetic field as well as energy-loss measurements, which contribute to charged particle identification. Surrounding the DCH is a detector of internally reflected Cherenkov radiation (DIRC), which provides charged hadron identification. Outside of the DIRC is a CsI(Tl) electromagnetic calorimeter (EMC) that is used to detect photons, provide electron identification, and reconstruct neutral hadrons. The EMC is surrounded by the superconducting coil, which creates the magnetic field for momentum and charge measurements. Outside of the coil, the flux return yoke is instrumented with resistive plate chambers interspersed with iron (IFR) for the identification of muons and long-lived neutral hadrons.

3 Candidate selection

$B^0 \to J/\psi\pi^0$ candidates are selected by identifying $J/\psi \to e^+e^-$ or $J/\psi \to \mu^+\mu^-$ decays and $\pi^0 \to \gamma\gamma$ decays (details are given in Ref. [5]). For the $J/\psi \to e^+e^-$ channel, photons consistent with bremsstrahlung are added and each lepton candidate must be consistent with the electron hypothesis. For the $J/\psi \to \mu^+\mu^-$ channel, each lepton candidate must be consistent with the muon hypothesis. The invariant mass of the lepton pair is required to be between 2.95 and 3.14 GeV/c^2, and 3.06 and 3.14 GeV/c^2, for the electron and muon channels, respectively. The photon candidates used to reconstruct the π^0 candidate are identified as clusters in the EMC within the polar angle range $0.410 < \theta_{\mathrm{lab}} < 2.409$ rad that are spatially separated from every charged track, and have a minimum energy of 30 MeV. The lateral energy distribution in the cluster is required to be consistent with a photon. The invariant mass of the photon pair is required to be $100 < m_{\gamma\gamma} < 160\,\mathrm{MeV}/c^2$. Finally, the J/ψ and π^0 candidates defined above are combined using a mass-constrained kinematic vertexing algorithm.

Two kinematic consistency requirements are applied to each B candidate. The difference, ΔE, between the B candidate energy and the beam energy in the center-of-mass frame must be $-0.4 < \Delta E < 0.4$ GeV. The beam-energy-substituted mass, $m_{\mathrm{ES}} = \sqrt{(E^*_{\mathrm{beam}})^2 - (p^*_B)^2}$, must be $5.2 < m_{\mathrm{ES}} < 5.3\,\mathrm{GeV}/c^2$, where E^*_{beam} and p^*_B are the beam energy and B candidate momentum in the center-of-mass frame.

Several kinematic and topological variables are linearly combined using a Fisher discriminant, $\mathcal{F}$, to provide additional separation between signal and $e^+e^- \to u\overline{u}, d\overline{d}, s\overline{s}, c\overline{c}$ (continuum) background events. The inputs to the Fisher discriminant are: the zeroth and second order Legendre polynomial momentum moments ($L_0 = \sum_i |\mathbf{p}_i|$ and $L_2 = \sum_i |\mathbf{p}_i| \frac{3\cos^2\theta_i - 1}{2}$, where $\mathbf{p}_i$ are the momenta for the charged and neutral objects in the event that are not associated with the signal candidate, and θ_i are the angles between $\mathbf{p}_i$ and the thrust axis of the signal candidate); the ratio of the second-order to zeroth-order Fox-Wolfram moment [8], computed using all charged and neutral objects not

Table 1: The efficiencies for the requirement on the Fisher discriminant and tagging, given independently, with statistical uncertainties.

Source type	Efficiency (%) of $\mathcal{F} > -0.8$	Tagging efficiency (%)
$B^0 \to J/\psi \pi^0$	99.2 ± 0.1	65.6 ± 0.6
$B^0 \to J/\psi K^0_S(\pi^0\pi^0)$ background	98.9 ± 0.1	65.6 ± 0.6
$B \to J/\psi$ X (inclusive J/ψ) background	94.9 ± 0.7	70.4 ± 1.4
$B \to$ X ($B\overline{B}$ generic) background	98.5 ± 0.4	61.1 ± 1.6
$e^+e^- \to q\overline{q}$ (continuum) background	28.6 ± 0.7	52.3 ± 0.8

associated with the signal candidate; $|\cos\theta_T|$, where θ_T is the angle between the thrust axis of the B candidate and the thrust axis of the remaining charged tracks and neutral objects in the event; $|\cos\theta_\ell|$, where θ_ℓ is the lepton helicity angle, defined as the angle between the negative lepton and B candidate directions in the J/ψ rest frame. We require $\mathcal{F} > -0.8$, which is 99% efficient for signal and rejects 71% of the continuum background. The efficiencies for satisfying this requirement are summarized in Table 1.

4 Backgrounds

The backgrounds come from decays which contain a J/ψ particle or from purely random combinations. We split the backgrounds into four categories.

One of the $B \to J/\psi$ X decays is $B^0 \to J/\psi K^0_S(\pi^0\pi^0)$. In this case, one of the π^0's is emitted nearly at rest in the center-of-mass frame, and is thus missed in the reconstruction of the B candidate. The second is the more general class of $B \to J/\psi$ X (inclusive J/ψ) decays, which contribute through random combinations of J/ψ and π^0 candidates. This also includes cascade decays through other charmonium states, but excludes the specific $B^0 \to J/\psi K^0_S(\pi^0\pi^0)$ mode discussed above. Third is a purely combinatoric background contribution coming from the general decay $B \to$ X ($B\overline{B}$ generic). Excluded from this definition are those decays already considered above. The fourth type of background is a combinatoric background due to u, d, s, and c quark production following the e^+e^- annihilation, $e^+e^- \to q\overline{q}$ (continuum). We study this background using an inverted lepton particle identification selection on the below-resonance data sample. In this case, the J/ψ candidate is reconstructed from two particle candidates that are not consistent with a lepton hypothesis. Monte Carlo simulation is used to check that this procedure correctly models the background.

5 Flavor tagging and measurement of Δt

The methods for B flavor tagging, vertex reconstruction, and the determination of Δt, are described in Refs. [3, 9]. For flavor tagging, we exploit information from the recoil B decay in the event. The charges of energetic electrons and muons from semileptonic B decays, kaons, soft pions from $D^{*+} \to D^0 \pi^+$ decays, and high momentum particles are correlated with the flavor of the decaying B meson. For B decays, about 66% of the events can be assigned to one of four hierarchical, mutually exclusive tagging categories. The remaining untagged events are excluded from further analysis. The total tagging efficiency for each source type is shown in Table 1.

The time interval Δt between the two B decays is calculated from the measured separation Δz between the decay vertex of the reconstructed B meson ($B_{\rm rec}$) and the vertex of the flavor-tagging B meson ($B_{\rm tag}$) along the beam axis (z axis). The calculation of Δt includes an event-by-event correction for the direction of the $B_{\rm rec}$ with respect to the z direction in the $\Upsilon(4S)$ frame. We determine the z position of the $B_{\rm rec}$ vertex from the reconstructed vertex of the J/ψ candidate. The $B_{\rm tag}$ vertex is determined by fitting the tracks not belonging to the $B_{\rm rec}$ candidate to a common vertex. An additional constraint on the tagging vertex comes from a pseudo-track computed from the $B_{\rm rec}$ vertex and three-momentum, the beam-spot (with a vertical size of $10\,\mu$m), and the $\Upsilon(4S)$ momentum. For 99.5% of the reconstructed events the r.m.s. Δz resolution is $180\,\mu$m. Convergence is required for both the $B_{\rm rec}$ and $B_{\rm tag}$ vertex fits. Finally, Δt must be between -20 and $20\,$ps, and it is required to have an uncertainty satisfying $\sigma_{\Delta t} < 2.4$ ps.

6 Maximum likelihood fitting technique

We extract the *CP* asymmetry by performing an unbinned extended likelihood fit. The likelihood is constructed from the probability density functions for the discriminating variables $m_{\rm ES}$, ΔE, and Δt. The quantity that is maximized is

$$\begin{aligned}\mathcal{L} = \frac{e^{-\sum_{j=1}^{5} n_j}}{N!} \prod_{i=1}^{N} \{ & f_\alpha^{Sig}\ n_{Sig}\ \mathcal{P}_{m_{\rm ES}}^{Sig}\ \mathcal{P}_{\Delta E}^{Sig}\ \mathcal{P}_{\Delta t}^{Sig} \\ & + f_\alpha^{Ks}\ n_{Ks}\ \mathcal{P}_{m_{\rm ES}-\Delta E}^{Ks}\ \mathcal{P}_{\Delta t}^{Ks} \\ & + f_\alpha^{Inc}\ n_{Inc}\ \mathcal{P}_{m_{\rm ES}-\Delta E}^{Inc}\ \mathcal{P}_{\Delta t}^{Inc} \\ & + f_\alpha^{BB}\ n_{BB}\ \mathcal{P}_{m_{\rm ES}}^{BB}\ \mathcal{P}_{\Delta E}^{BB}\ \mathcal{P}_{\Delta t}^{BB} \\ & + f_\alpha^{Cont}\ n_{Cont}\ \mathcal{P}_{m_{\rm ES}}^{Cont}\ \mathcal{P}_{\Delta E}^{Cont}\ \mathcal{P}_{\Delta t}^{Cont}\},\end{aligned} \tag{3}$$

where n_j is the number of events for each of the 5 hypotheses (1 signal and 4 backgrounds) and N is the number of input events. The $\mathcal{P}$ are the probability density functions (PDFs) for each discriminating variable and signal or background type. The parameters f_α^j are the tagging efficiencies for each of the 4 tagging categories α and each of the signal or background types j. For the $B^0 \to J/\psi\,\pi^0$ signal and $B^0 \to J/\psi\,K_S^0(\pi^0\pi^0)$ background, the values of f_α^j are measured with a sample ($B_{\rm flav}$) of neutral B decays to flavor eigenstates consisting of the channels $D^{(*)-}h^+(h^+ = \pi^+, \rho^+$, and $a_1^+)$ and $J/\psi\,K^{*0}(K^{*0} \to K^+\pi^-)$ [3]. For the inclusive J/ψ background and $B\overline{B}$ generic background, they are measured with Monte Carlo simulation [10], and for the continuum background, they are measured with the inverted lepton particle identification data sample. We discuss the discriminating variables ($m_{\rm ES}$, ΔE, and Δt) in the following sections.

6.1 Probability density functions for $m_{\rm ES}$ and ΔE

The signal $m_{\rm ES}$ distribution is modeled as the sum of two components. The first is a modified Gaussian function which, for values less than the mean, has a width parameter that scales linearly with the distance from the mean. The second component, accounting for less than 6% of the distribution, is an ARGUS function [11], which is a phase-space distribution of the form

$m_{\mathrm{ES}}\sqrt{(1-\frac{m_{\mathrm{ES}}{}^2}{E_{beam}^2})}\exp(\xi(1-\frac{m_{\mathrm{ES}}{}^2}{E_{beam}^2}))$, with a kinematic cut-off at $E_{beam} = 5.289\,\mathrm{GeV}$, and one parameter to fit in the exponential, ξ. The signal ΔE distribution is modeled by the sum of a Crystal Ball function [12] and a second order polynomial. The Crystal Ball function is defined as

$$C(\Delta E) = \begin{cases} e^{-\frac{(\Delta E-m)^2}{2\sigma^2}} & \text{if } \Delta E > m-\alpha\sigma \\ \frac{(\frac{n}{\alpha})^n \; e^{-\frac{\alpha^2}{2}}}{(\frac{m-\Delta E}{\sigma}+\frac{n}{\alpha}-\alpha)^n} & \text{if } \Delta E \leq m-\alpha\sigma, \end{cases} \tag{4}$$

where m is the position of the maximum. The parameter α determines the cross-over point from a Gaussian behavior to a power-law, and is expressed in units of the peak width σ. The parameter n is a real number which enters into the power-law portion of the function. The parameters of these PDFs are determined by fitting to a signal Monte Carlo sample. The maximum of the ΔE distribution is a free parameter of the full *CP* likelihood fit to allow for EMC energy scale uncertainties.

The kinematic variables m_{ES} and ΔE are correlated for the $B^0 \rightarrow J/\psi\, K^0_S(\pi^0\pi^0)$ and the inclusive J/ψ backgrounds. To account for this, 2-dimensional PDFs are employed. Variably binned interpolated 2-dimensional histograms of these variables are constructed from the relevant Monte Carlo samples.

The m_{ES} PDFs for the $B\overline{B}$ generic and continuum backgrounds are modeled by the ARGUS function and the ΔE PDFs for these two backgrounds are modeled by a second order polynomial. The parameters for these PDFs are obtained from the $B\overline{B}$ generic Monte Carlo sample and the inverted lepton particle identification data sample.

6.2 Probability density functions for Δt

The PDFs used to describe the Δt distributions of the signal and background sources are each a convolution of a resolution function $\mathcal{R}$ and decay time distribution $\mathcal{D}$: $\mathcal{P}(\Delta t) = \mathcal{R}(\Delta t) \otimes \mathcal{D}(\Delta t)$.

For the signal, the resolution function [9] consists of the sum of three Gaussians, which will be referred to as the core, tail, and outlier. The means of the Gaussians are biased away from zero due to the charm content of the side of the event used for tagging. For the core and tail Gaussians this bias is multiplied by the Δt per-event error $\sigma_{\Delta \mathrm{t}}$. The widths of the core and tail Gaussians are the products of the per-event errors and scale factors. The tail Gaussian has a fixed scale factor of 3 and the outlier Gaussian has a fixed width of 8 ps and zero mean. The five remaining parameters are measured with the large B_{flav} data sample. The bias of the core Gaussian has different values for each of the four tagging categories.

The decay time distribution is given by Eq. 1 modified for the effects of B flavor tagging:

$$\mathcal{D}^{\pm}_{\alpha,f}(\Delta t) = \frac{e^{-|\Delta t|/\tau_{B^0}}}{4\tau_{B^0}}\{(1 \mp \Delta w_\alpha) \pm S_f\;(1-2w_\alpha)\sin(\Delta m_d \Delta t) \\ \mp C_f\;(1-2w_\alpha)\cos(\Delta m_d\Delta t)\}, \tag{5}$$

where $\mathcal{D}^{+}_{\alpha,f}(\mathcal{D}^{-}_{\alpha,f})$ is for a $B^0(\overline{B}^0)$ tagging meson. The variable w_α is the average probability of incorrectly tagging a B^0 as a $\overline{B}^0$ ($w^{B^0}_\alpha$) or a $\overline{B}^0$ as a B^0 ($w^{\overline{B}^0}_\alpha$), and $\Delta w_\alpha = w^{B^0}_\alpha - w^{\overline{B}^0}_\alpha$. Both w_α

Table 2: Results of the *CP* likelihood fit. Errors are statistical only. The global correlation is 0.14 for $C_{J/\psi\pi^0}$ and 0.15 for $S_{J/\psi\pi^0}$. The projections of the PDFs are shown in Figure 1 and the asymmetry in Figure 2.

	Fit results
$C_{J/\psi\pi^0}$	0.38 ± 0.41
$S_{J/\psi\pi^0}$	0.05 ± 0.49
Signal ΔE Maximum (MeV)	-13.2 ± 7.2
$B^0 \to J/\psi\pi^0$ signal (Events)	40 ± 7
$B^0 \to J/\psi K^0_S(\pi^0\pi^0)$ background (Events)	140 ± 19
Inclusive J/ψ background (Events)	109 ± 35
$B\overline{B}$ generic background (Events)	52 ± 25
Continuum background (Events)	97 ± 22

and Δw_α are determined using the $B_{\rm flav}$ data sample [3]. The values of Δm_d and τ_{B^0} are the 2002 PDG averages [13].

The PDF used to model the Δt distribution for the $B^0 \to J/\psi K^0_S(\pi^0\pi^0)$ background takes the same form as that for signal, but with $S_{J/\psi K^0_S} = 0.75$ [14], and $C_{J/\psi K^0_S} = 0$.

The parameterizations of the Δt PDFs for the inclusive J/ψ background and the $B\overline{B}$ generic background consist of lifetime and prompt components. The resolution function for each component is the sum of core and outlier Gaussians, where the width of each core Gaussian is the product of $\sigma_{\Delta t}$ and a scale factor. Once again, the width and mean of the outlier Gaussians are fixed to 8 ps and zero respectively. For each of these background sources, the fraction which is in the lifetime component, the decay lifetime parameter, and the resolution parameters are the values determined from the Monte Carlo simulation.

The Δt PDF for the continuum background consists of a double Gaussian which has the same form as the prompt component of the inclusive J/ψ and $B\overline{B}$ generic Δt PDFs, where in this case the parameter values are obtained by fitting the inverted lepton particle identification data sample.

6.3 Results of the *CP* asymmetry fit

The results of the *CP* asymmetry fit to 438 events found in 81 fb^{-1} of data are shown in Table 2. The projections in $m_{\rm ES}$, ΔE, and Δt, are shown in Figure 1. Figure 2 shows the Δt distributions and asymmetries in yields between B^0 and $\overline{B}^0$ flavor tags as functions of Δt, overlaid with the projection of the likelihood fit results.

7 Systematic uncertainties

The contributions to the systematic errors in $C_{J/\psi\pi^0}$ and $S_{J/\psi\pi^0}$ are summarized in Table 3. The first class of uncertainties are those obtained by variation of the parameters used in the $m_{\rm ES}$, ΔE, and Δt PDFs, where the dominant sources are the uncertainties in the signal ΔE PDF parameters. Another contribution is due to the energy scale uncertainties in the modeling of the $B^0 \to J/\psi K^0_S(\pi^0\pi^0)$ background. An additional systematic uncertainty comes from altering the configuration of the 2-dimensional PDFs for the $B^0 \to J/\psi K^0_S(\pi^0\pi^0)$ and inclusive J/ψ backgrounds. A systematic error

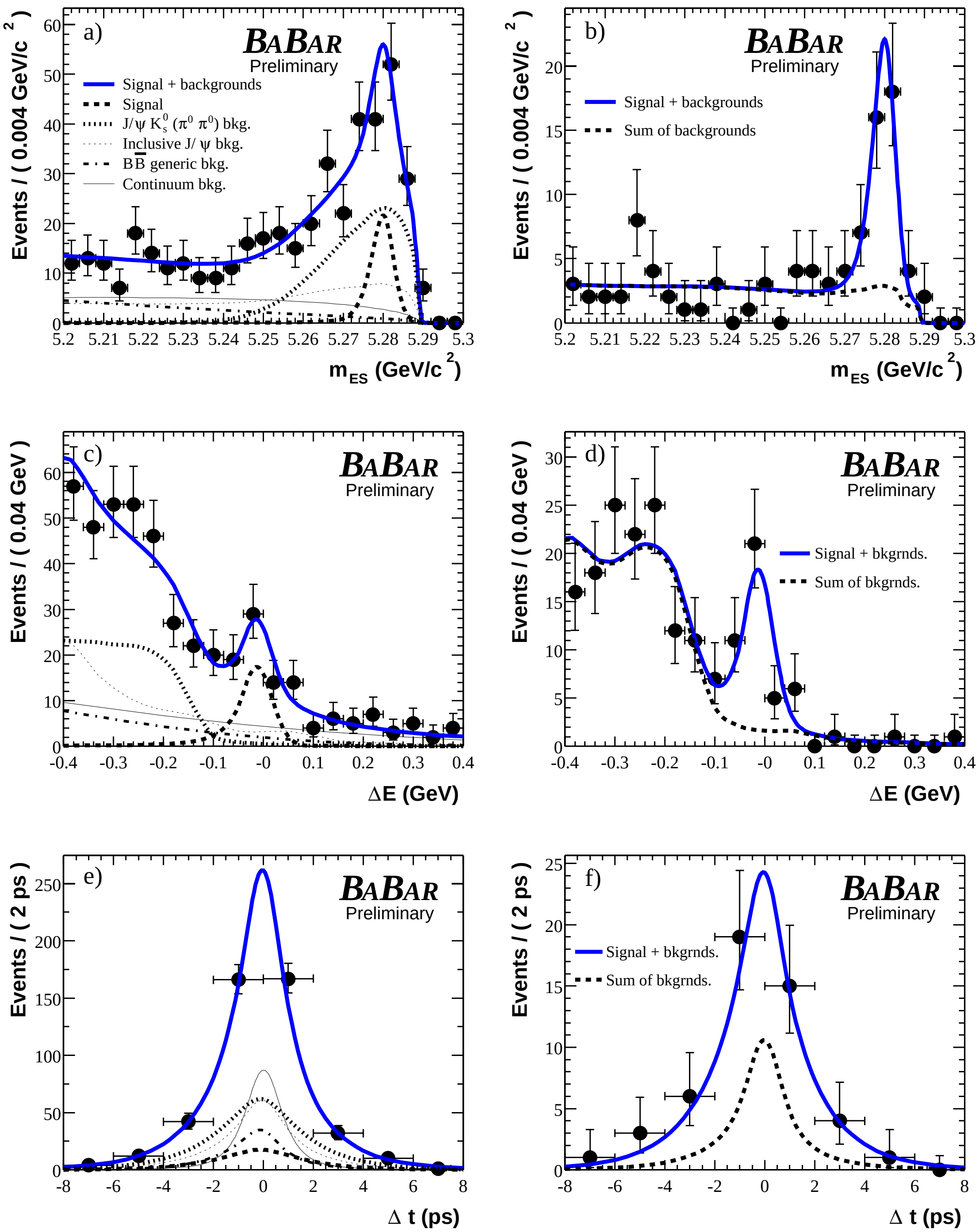

Figure 1: Projections in a) $m_{\rm ES}$, c) ΔE, and e) Δt for the results of the CP fit to $81\,{\rm fb}^{-1}$ of data. The legend in a) applies to the plots on the left hand side. The projection in b) $m_{\rm ES}$ is shown with the requirement $-0.11 < \Delta E < 0.11\,{\rm GeV}$. The projection in d) ΔE is shown with the requirement $m_{\rm ES} > 5.27\,{\rm GeV}/c^2$. The projection in f) Δt is shown with the requirements $-0.11 < \Delta E < 0.11\,{\rm GeV}$ and $m_{\rm ES} > 5.27\,{\rm GeV}/c^2$. These plots do not represent the full information used in the maximum likelihood fit, but only a partial view of the data.

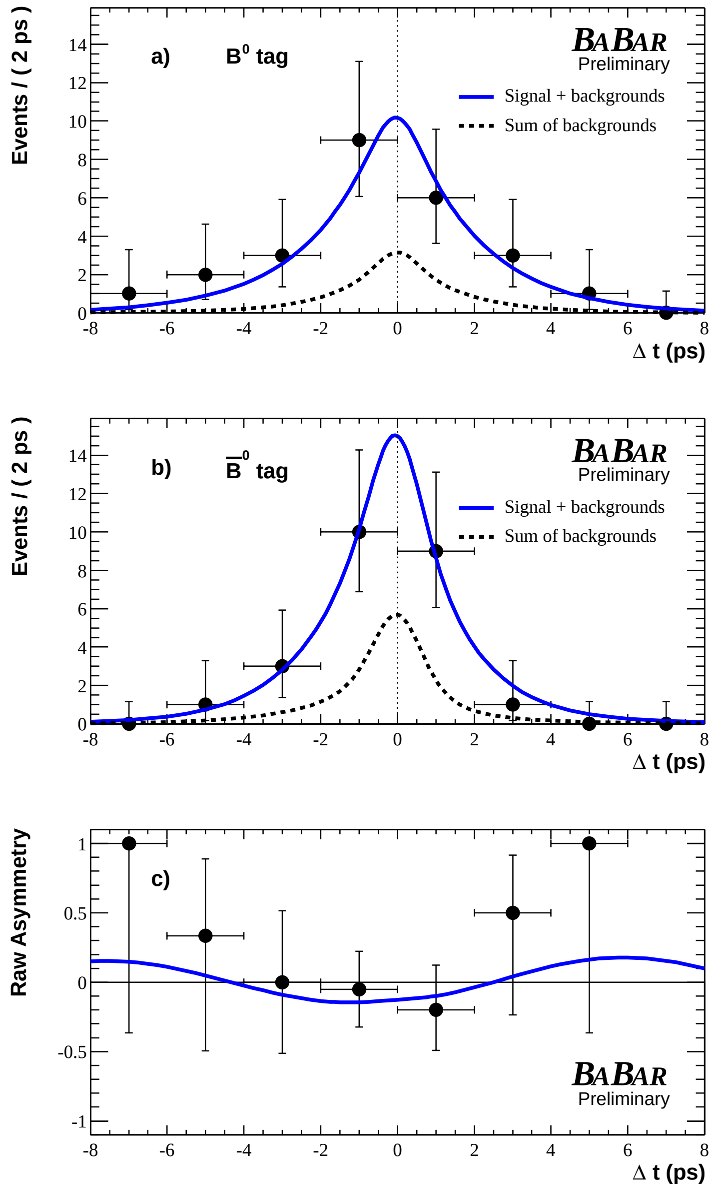

Figure 2: Number of candidates in the signal region a) with a B^0 tag N_{B^0} and b) with a $\overline{B}^0$ tag $N_{\overline{B}^0}$, and c) the raw asymmetry $(N_{B^0} - N_{\overline{B}^0})/(N_{B^0} + N_{\overline{B}^0})$, as functions of Δt. Candidates in these plots are required to satisfy $-0.11 < \Delta E < 0.11\,\mathrm{GeV}$ and $m_{\mathrm{ES}} > 5.27\,\mathrm{GeV}/c^2$. The curves in a) and b) are projections that use the values of the other variables in the likelihood to determine the contribution to the signal or one of the backgrounds.

Table 3: Summary of the systematic errors.

Source	Error on $C_{J/\psi\,\pi^0}$	Error on $S_{J/\psi\,\pi^0}$
Parameter variations		
$m_{\rm ES}$ and ΔE parameters	0.048	0.130
Tagging fractions	0.002	0.007
Δt parameters	0.027	0.022
Additional systematics		
EMC energy scale $B^0 \to J/\psi\, K^0_S(\pi^0\pi^0)$	0.009	0.002
Changing the 2-D histogram PDFs	0.009	0.029
Using 2-D PDF for signal	0.073	0.079
Beam spot, boost/vtx., SVT misalign.	0.012	0.012
Total systematic uncertainty	0.093	0.157

to account for a correlation between the tails of the signal $m_{\rm ES}$ and ΔE distributions is obtained by using a 2-dimensional PDF.

8 Summary

An unbinned extended maximum likelihood fit has been performed on $81\,{\rm fb}^{-1}$ of data collected at *BABAR*, yielding preliminary values for the coefficients of the cosine and sine terms of the time-dependent *CP* asymmetry in $B^0 \to J/\psi\,\pi^0$ decays:

$$C_{J/\psi\,\pi^0} = 0.38 \pm 0.41\ ({\rm stat}) \pm 0.09\ ({\rm syst}),$$
$$S_{J/\psi\,\pi^0} = 0.05 \pm 0.49\ ({\rm stat}) \pm 0.16\ ({\rm syst}).$$

9 Acknowledgments

We are grateful for the extraordinary contributions of our PEP-II colleagues in achieving the excellent luminosity and machine conditions that have made this work possible. The success of this project also relies critically on the expertise and dedication of the computing organizations that support *BABAR*. The collaborating institutions wish to thank SLAC for its support and the kind hospitality extended to them. This work is supported by the US Department of Energy and National Science Foundation, the Natural Sciences and Engineering Research Council (Canada), Institute of High Energy Physics (China), the Commissariat à l'Energie Atomique and Institut National de Physique Nucléaire et de Physique des Particules (France), the Bundesministerium für Bildung und Forschung and Deutsche Forschungsgemeinschaft (Germany), the Istituto Nazionale di Fisica Nucleare (Italy), the Foundation for Fundamental Research on Matter (The Netherlands), the Research Council of Norway, the Ministry of Science and Technology of the Russian Federation, and the Particle Physics and Astronomy Research Council (United Kingdom). Individuals have received support from the A. P. Sloan Foundation, the Research Corporation, and the Alexander von Humboldt Foundation.

References

[1] N. Cabibbo, Phys. Rev. Lett. **10**, 531 (1963);
M. Kobayashi and T. Maskawa, Prog. Th. Phys. **49**, 652 (1973).

[2] *BABAR* Collaboration, B. Aubert *et al.*, Phys. Rev. Lett. **87**, 091801 (2001).

[3] *BABAR* Collaboration, B. Aubert *et al.*, SLAC-PUB-9293, hep-ex/0207042, submitted to Phys. Rev. Letters.

[4] Belle Collaboration, K. Abe *et al.*, Phys. Rev. Lett. **87**, 091802 (2001).

[5] *BABAR* Collaboration, B. Aubert *et al.*, Phys. Rev. D **65**, 032001 (2002).

[6] See, for example, L. Wolfenstein, Eur. Phys. Jour. C **15**, 115 (2000).

[7] *BABAR* Collaboration, B. Aubert *et al.*, Nucl. Instr. Methods **A479**, 1 (2002).

[8] G. C. Fox and S. Wolfram, Nucl. Phys. **B149**, 413 (1979).

[9] *BABAR* Collaboration, B. Aubert *et al.*, SLAC-PUB-9060, hep-ex/0201020, submitted to Phys. Rev. D.

[10] Geant4 Collaboration, CERN-IT-2002-003, submitted to Nucl. Instr. Methods **A**.

[11] ARGUS Collaboration, H. Albrecht *et al.*, Phys. Lett. B **185**, 218 (1987); **241**, 278 (1990).

[12] Crystal Ball Collaboration, D. Antreasyan *et al.*, Crystal Ball Note 321 (1983).

[13] Particle Data Group, K. Hagiwara *et al.*, Phys. Rev. D **66**, 010001 (2002).

[14] *BABAR* Collaboration, B. Aubert *et al.*, presented at Les 16iemes Rencontres de Physique de la Vallee d'Aoste, *BABAR*-CONF-02/01, hep-ex/0203007 (2002).